RECENT PROGRESS IN SCRAMJET / ROCKET BASED COMBINED CYCLE ENGINES AT JAXA, KAKUDA SPACE PROPULSION CENTER

S. Ueda, S. Sato, K. Itoh, K. Tani, S. Tomioka and T. Kanda
JAXA, Combined Propulsion Research Group
1 Koganesawa, Kimigaya, Kakuda, Miyagi 981-1525 Japan

OVERVIEW

This report presents recent research activities of the Combined Propulsion Research Group of Japan Aerospace Exploration Agency. Aerodynamics and combustion of the scramjet engine and the rocket-ramjet combined-cycle engine, structure and material for the two engines and thermo-aerodynamic of a re-entry vehicle are major subjects. In Mach 6 condition tests, a scramjet engine model produced about 2000 N net thrust, whereas a model produced thrust almost equal to its drag in Mach 12 condition. A rocket-ramjet combined-cycle engine model was fabricated and was tested under sea-level, static conditions. Studies of combustor models and aerodynamic component models were conducted for demonstration of the engine operation and improvement of its performances. Light-weight cooling panel by electrochemical etching examined and C/C composite cooling structure was investigated. Thermo-aerodynamics of re-entry vehicle was investigated and measurement technique was developed in high enthalpy flow.

1. INTRODUCTION

An orbital vehicle needs large kinetic energy. Conventional liquid rockets attain this speed with consumption of onboard oxidizer such as liquid oxygen, which is about 70% of initial weight of the rockets. Air-breathing engines use oxygen in air and implementation of the engine to a launch vehicle will cause larger payload to an orbit. The scramjet engine, a hypersonic air-breathing engine, has a high performance in hypersonic speed, and its application to a booster stage will increase payload to an orbit, comparing to that by the conventional space transportation systems. The Combined Propulsion Research Group of Japan Aerospace Exploration Agency (JAXA), Kakuda Space Propulsion Center (KSPC) has progressed research on a scramjet engine to establish its design technologies from 1980s.[1],[2]

The scramjet engine can operate only in the hypersonic speed and needs other engines to flight in other conditions, such as taking-off and space flight. To obtain larger operability, the group has started to study a rocket-ramjet combined-cycle engine. The rocket-ramjet combined-cycle engine is a combination of the rocket engine and the ramjet engine.[3] This engine has rocket engines inside the ramjet engine duct and can operate from take-off to orbital flight. Figure 1 shows an image of the engine and Figure 2 shows a series of operating schematics of the engine. The engine operates in the ejector-jet mode in low speed. As flight speed increases, its operating mode changes to the ramjet, the scramjet and the rocket.[4],[5] In order to change these operating modes, the engine should be a variable geometry configuration. However, this complicated configuration will make many kinds of difficulties in its development, maintenance and cost. Fixed geometry engine is presumed in the research activities in this group. In the present paper, recent progresses of scramjet and combined-cycle engine research works in JAXA-KSPC are presented.

2. RESEARCH HISTORY IN KSPC

Figure 3 shows the diagram of our research activities for the scramjet and combined cycle engines. Prior to the activities listed in the figure, a study of the air-breathing rocket (ABR) started in 1975.[6] Around 1980s, component and system studies on the scramjet engine started. For further research activities in 1990s, three major facilities were constructed; the Ramjet Engine Test Facility (RJTF), the Numerical Space Engine (NSE), and the High Enthalpy Shock Tunnel (HIEST). At RJTF, sub-scale engine combustion tests can be conducted in hypersonic flight condition from Mach 4 to 8. At HIEST, tests at higher Mach number flight conditions can be operated. The NSE, the supercomputer system for the combined cycle engine, can simulate operating conditions of the engine models tested at RJTF, HIEST and other small facilities. Table 1 lists specifications of the facilities. RJTF was recently modified to conduct Mach 0 condition test, that is, the sea-level still air condition test for the ejector-jet mode tests. The design technology of the ejector-jet mode can be applied to a booster engine of a rocket vehicle. The technologies of the dual-mode scramjet engine can be also applied to a hypersonic flight vehicle.[7]

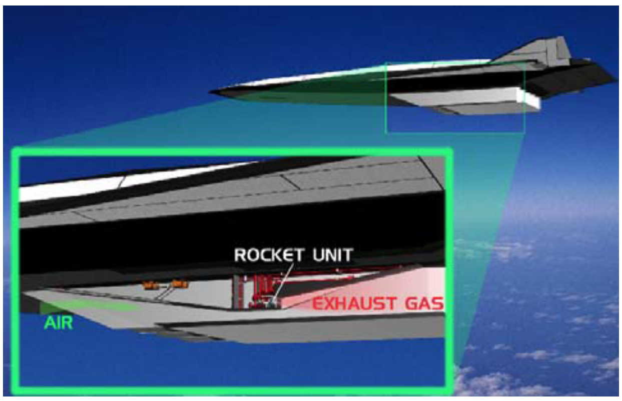

FIG 1. Image of Rocket-ramjet combined-cycle engine.

TAB 1. Features of RJTF, HIEST and NSE.

RJTF	M4 and 6 at dynamic press. 50 kPa M8 at dynamic press. 25 kPa
HIEST	Maximum stagnation enth. 25 MJ/kg Maximum stagnation press. 150 MPa
NSE	512 Gflops, 512 GB memory, 64 CPU

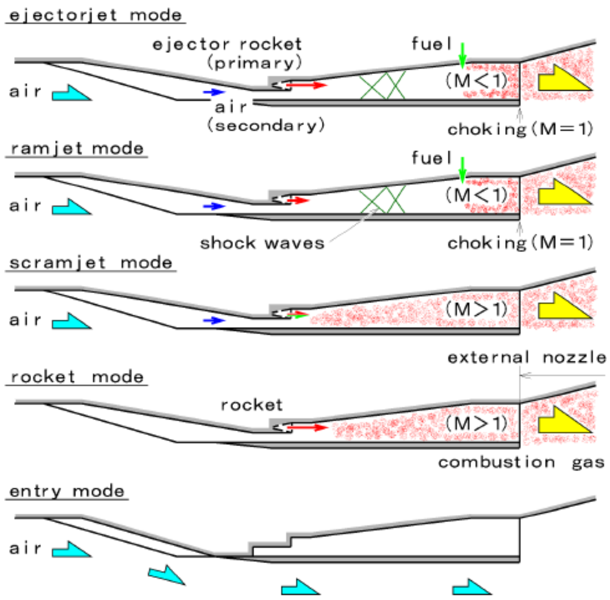

FIG 2. Conceptual Operating modes of rocket-ramjet combined-cycle engine.

3. SCRAMJET ENGINE STUDIES

Studies on the scramjet engine, preceding studies to those on the combined-cycle engine, have produced remarkable results in experimental, numerical and system investigations. Recent activities are introduced in this section. From March to April of 2005, a scramjet engine model (E2) was tested under Mach 6 flight condition at RJTF. Staged fuel injection was tried and an effect of inflow boundary layer was investigated.[8],[9] Figure 4 shows a schematic of the engine model, and Figure 5 shows thrust increment against an equivalence ratio (Φ) with the boundary-layer bleeding. Fuel was injected from a strut (SV1), and three positions on the sidewalls indicated with MV1, MV3 and MV4. While first stage fuel injection (MV1 or SV1) was fixed to Φ = 0.50, the second-stage fuel injection (MV3) was increased. Un-start transition did not occur with boundary layer bleeding up to Φ = 1.45. The engine model produced about 1.9 kN net thrust and specific impulse of 9000 $m \cdot s^{-1}$. The net thrust doubled the previous value by the single fuel injection. Figure 6 shows numerical simulation results with NSE, showing OH distributions at fuel flow rates.[10] In HIEST, another scramjet engine model was tested under hypervelocity conditions over Mach 10 flight.[11] One of the technical issues causing a severe drop in scramjet combustor performance at hypervelocity over Mach 10 flight is loss in net combustion heat release due to thermal dissociation of the combustion gas as a result of an increase in the combustion gas temperature. To improve the scramjet combustor performance at hypervelocity, we began to investigate the possibility of optimizing the combustion gas temperature to minimize loss in the net heat release.

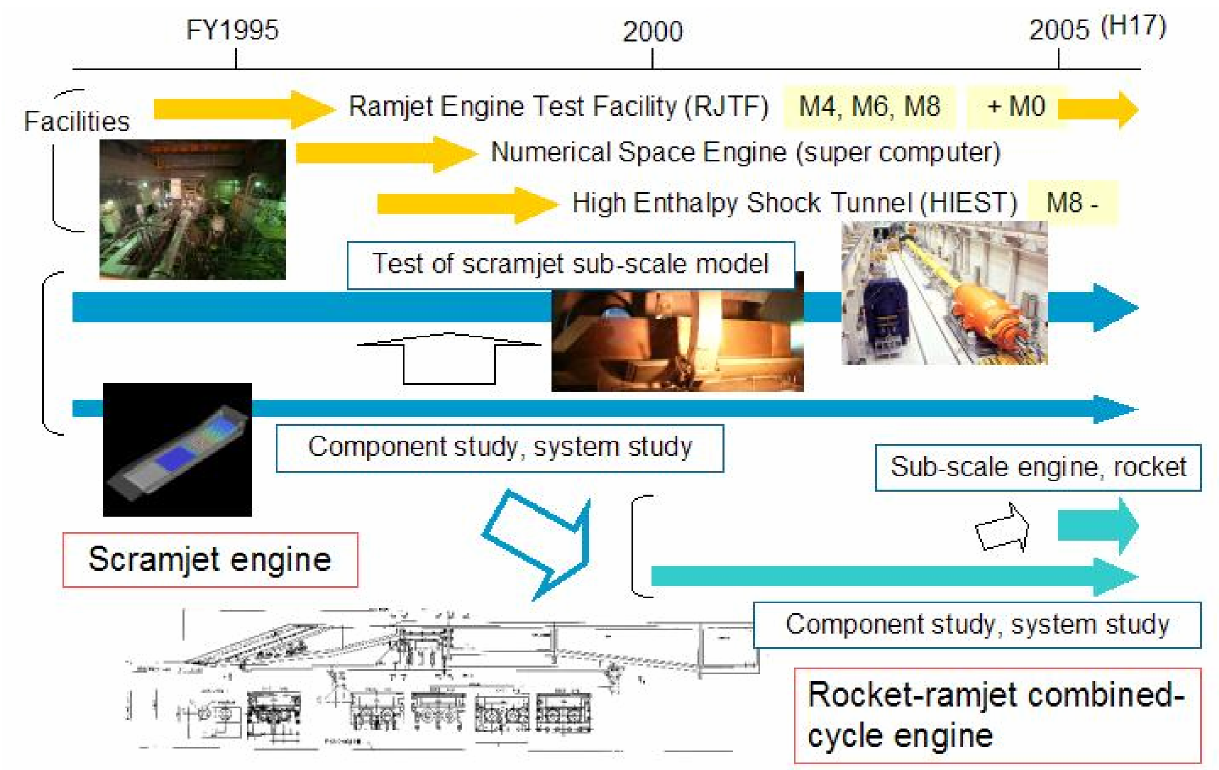

FIG 3. Research activities on scramjet and combined-cycle engines in JAXA-KSPC.

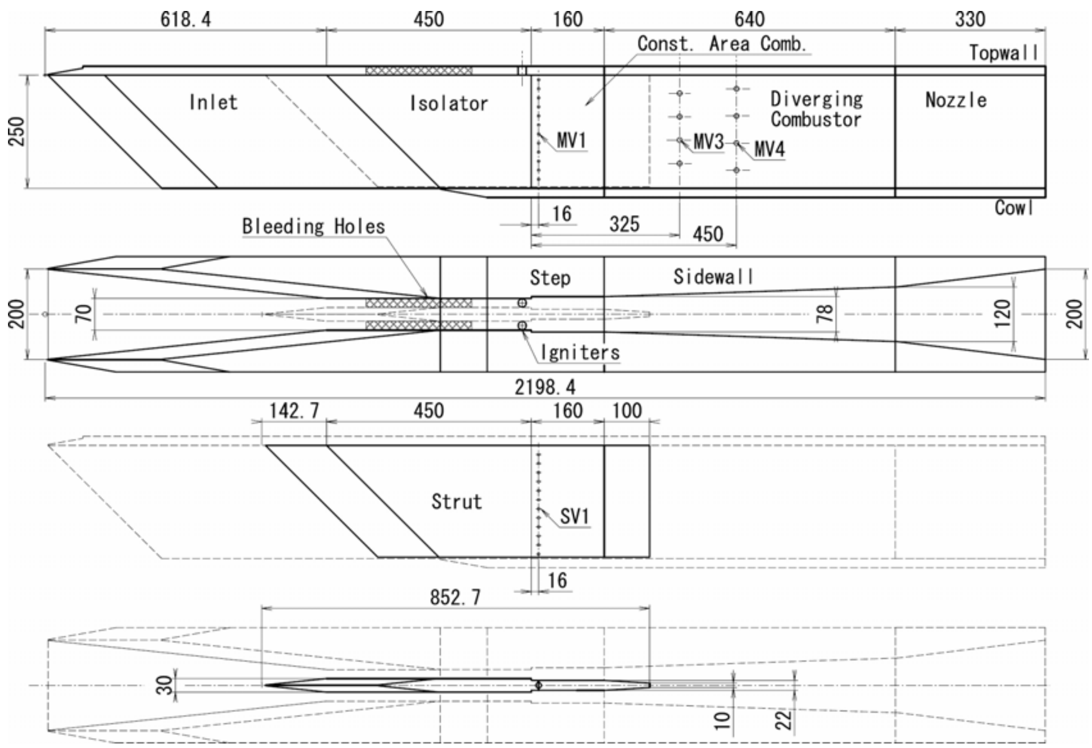

FIG 4. Schematic of scramjet engine model tested under Mach 6 condition at RJTF.

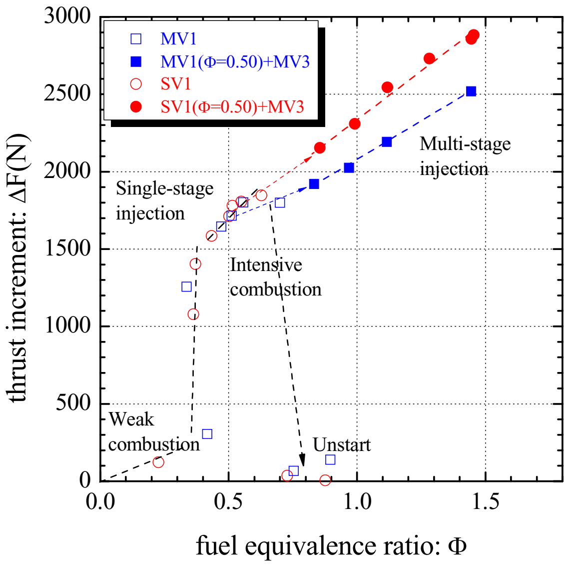

FIG 5. Thrust increment of scramjet model under Mach 6 condition at RJTF.

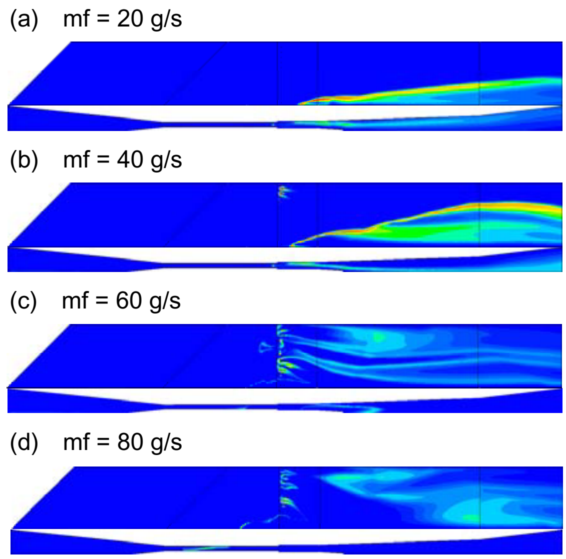

FIG 6. OH distributions in scramjet engine model at Mach 6 condition of RJTF.

The modified scramjet engine models M12-01, M12-02 and M12-03 were designed and were tested in the HIEST.[12] Figure 7 shows a schematic of the M12-03 engine. In Figure 8, the increment of the specific impulse due to combustion (ΔIsp) was compared with those obtained with the previous engines. It showed a remarkable improvement in ΔIsp at the enthalpy condition of 7MJ/kg or higher.

4. ROCKET-RAMJET COMBINED CYCLE ENGINE STUDIES

4.1. Engine model for RJTF tests

A rocket-ramjet combined cycle engine model, shown in Figure 9, embedding twin rocket chamber on top wall side of a scramjet flow pass, was fabricated and was tested under sea-level, static conditions.[13]

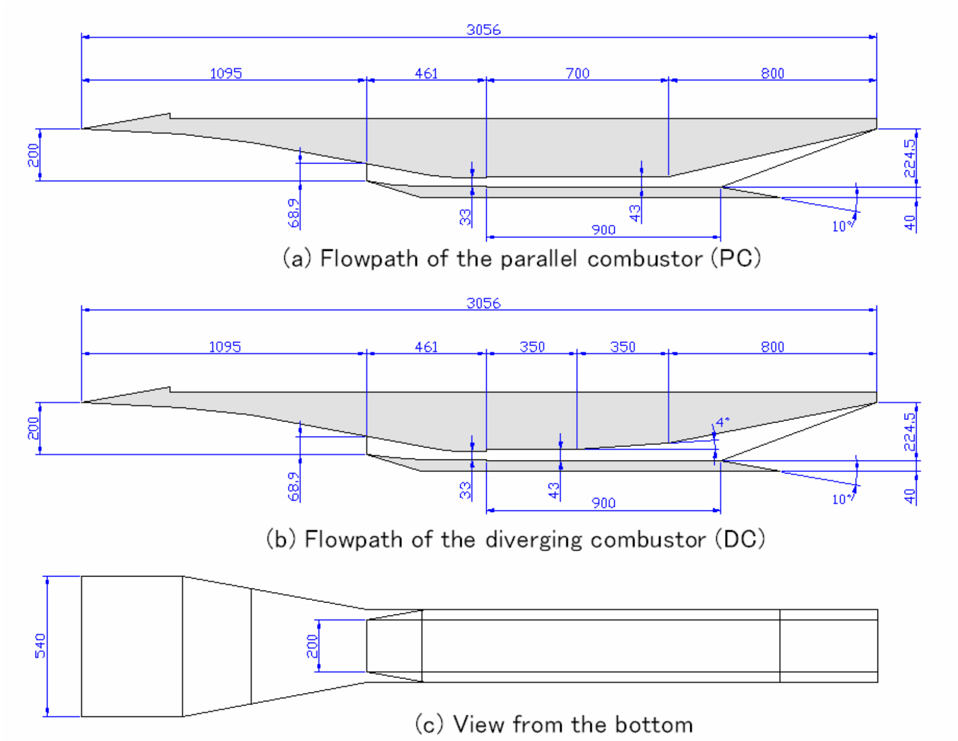

FIG 7. Schematic of the M12-03 engine.

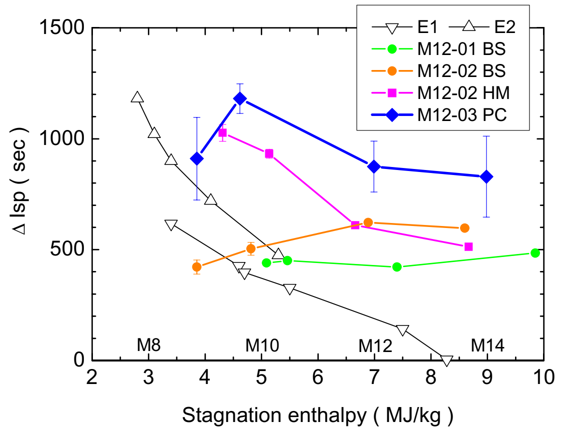

FIG 8. Comparison of the increment of specific impulse due to combustion (ΔIsp).

The rocket chamber was driven with gaseous hydrogen and oxygen at nominal operation condition of 3 MPa in chamber pressure and 7.5 in mixture ratio. Figure 10 shows the firing test of the clustered rocket chamber.[14] As the plume was over-expanded, a shock train was formed to recover the flow pressure. Gaseous hydrogen was also injected through secondary injector orifices to pressurize the ramjet combustor. Contraction in the inlet section was changed to investigate air ingestion performance, while a mechanical contraction mechanism with variable contraction ratio was installed near the exit of the engine to enhance pressure recovery within the diverging portion of the flow pass. The variety of cowl design being shown in Figure 11. The standard configuration was the drooped geometry to attain good capture in both high and low airspeed regime. The contracting geometry was to attain choked condition of the airflow before entering the following combustor sections, however, airflow rate was supposed to reduced as the flow pass cross-sectional area was squeezed.

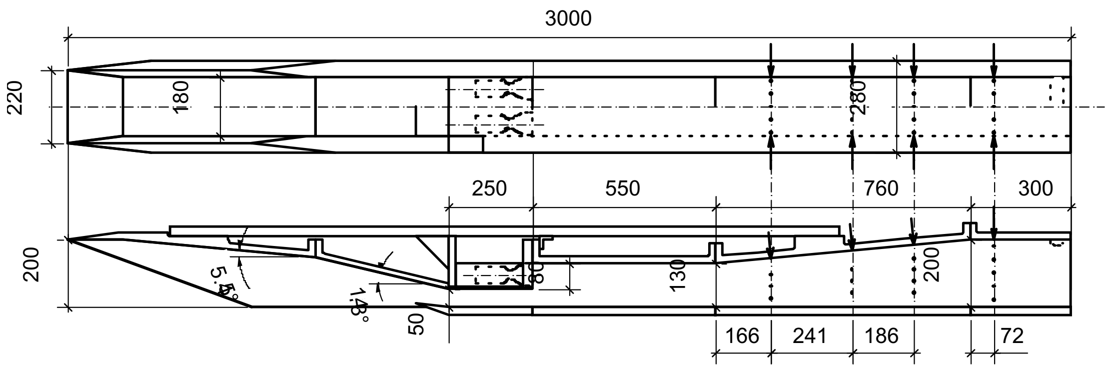

FIG 9. Schematic of rocket-ramjet combined-cycle engine model.

The stretched flat geometry was to attain higher contraction than the drooped cowl without sacrificing the flow pass cross-sectional area. The stretched contracting geometry provided highest contraction ratio among all. Test results showed that choking of the ingested airflow was not attained, and the airflow rate was 2/3 of the design value. Pressure-rise within the diverging portion of the flow pass was not intensive to attain choked condition at the engine exit. An excess injection of secondary fuel generated a shock system-like pressure rise, however, enhanced mixing was not sufficient to sustain pressure-rise through secondary combustion within the ramjet combustor with the excessive injection turned-off. Thus, enhancement of mixing between the airflow and rocket plume without help of the shock system is necessary for further thrust augmentation.

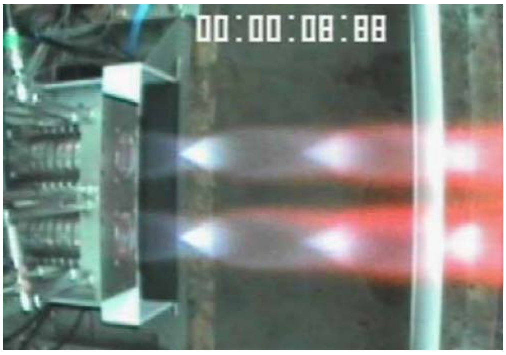

FIG 10. Water-cooled clustered rocket chamber for a rocket-ramjet combined cycle engine.

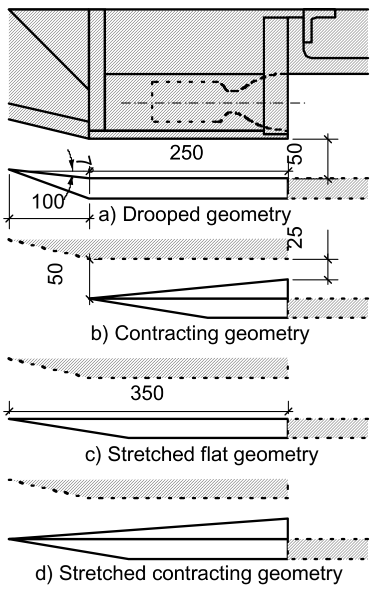

FIG 11. Cowl leading edge configurations.

4.2. Component studies

Prior to the test in RJTF, component tests were conducted to demonstrate the operation of the combined-cycle engine and these experimental results were used to design the RJTF model. Figure 12 shows an example of wall pressure distributions of a combustor model in the ejector-jet mode at sea-level, still-air condition.[15] Breathed air was choked at the exit of the throat section. Pressure became lower than the choking pressure of an atmospheric air around the entrance of the divergent section. The combustion gas choked at the exit of the model. Figure 13 shows wall pressure distributions in the downstream-combustion ramjet mode.[16] In this mode, fuel is injected into the downstream combustor. Subsonic combustion and subsequent choking at the exit are attained. The inlet section should satisfy contradicting requirements; sufficient air capture in the subsonic and transonic condition and sufficient compression in the supersonic and hypersonic condition. Experimental and numerical investigations were conducted to design the engine model. Figure 14 shows CFD results of the inlet sections at Mach 10.[17] The shock waves from the side wall leading edges deformed the ramp shock around the symmetric plane, and this interaction increased spillage. The engine operation was examined in a transonic wind tunnel. Figure 15 shows a wind tunnel model.[18] Nitrogen gas was used to simulate rocket exhaust. The ejector-jet mode operation was demonstrated and aerodynamic improvements were achieved.

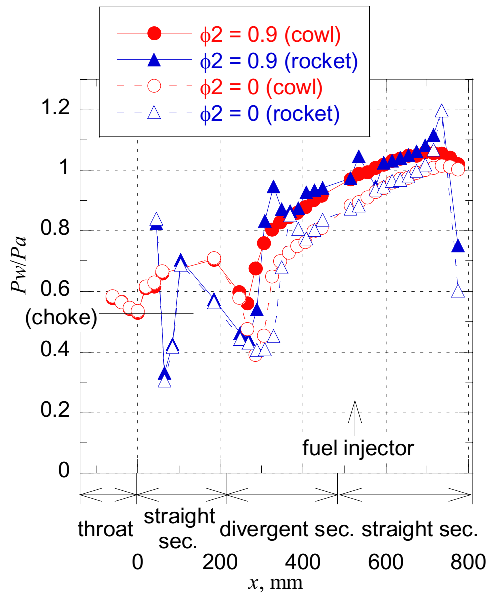

FIG 12. Wall pressure distributions in ejector-jet mode combustor model.

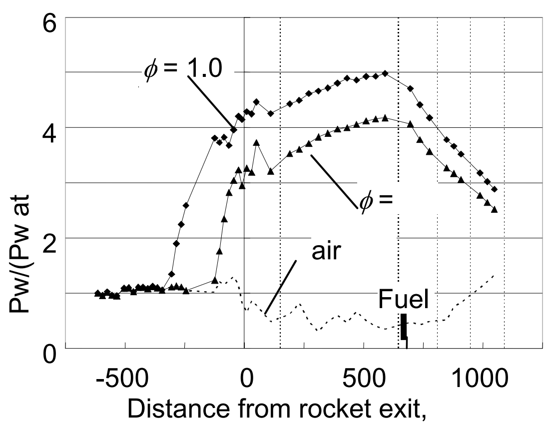

FIG 13. Wall pressure distributions in a combustor model.

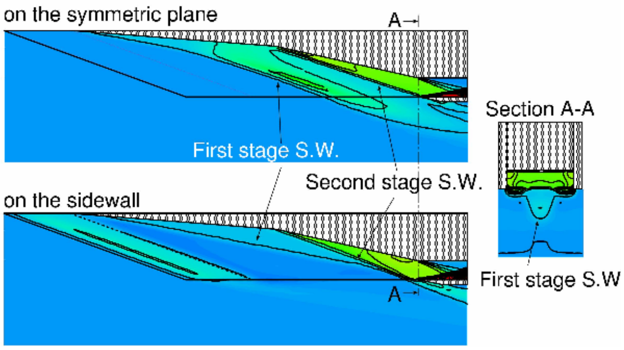

FIG 14. Isobars in inlet section.

5. FUNDERMENTAL RESEARCH WORKS

5.1. Cooling Structure and Material

As shown in Fig. 1, the scramjet engine and the combined-cycle engine have a large duct for air and combustion gas. Therefore, light-weight structure and material are required. The engines require the regenerative cooling and the cooling system is composed of large panels.In this group, production technique of the large cooling panel and light-weight material of C/C composite have been investigated. Machining to such a large panel will be difficult. Electrochemical etching was employed for creating cooling passages on the nickel alloy plate.[19],[20] Figure 16 is a picture of the plate after etching. The passages were etched into the entire plate as shown in this figure. Figure 17 shows details of the three-dimensional shape of the passages. These figures indicate that the passages at the edge were deeper than those in the center area and that the ribs between passages at the edge were narrower than those at in the center area. It was occurred due to the nonuniform current distribution on the plate.

Application of Carbon/Carbon (C/C) composite, which has a superior specific strength under conditions of high temperature. However, its practical use has been limited, the main problems facing utilization being 1) oxidation, 2) gas leakage, and 3) bonding. A coating will be able to improve the oxidation-resistance and airtightness of this composite in the near future. Its lifetime, however, depends on the heat-resistance of the coating. Furthermore, the heat-resistance temperature of junction partner materials, the thermal stress at the junction, and the heat-resistant nature of the parts used for the junction are problematic. A new cooling structure for C/C composites in which stainless steel tubes are fixed by the elastic forces of the material as shown in Fig. 18, was proposed.[21],[22] A specimen was heated by infrared rays from a lamp. Sufficient cooling performance of such a structure was obtained. A rocket combustor was also used for evaluation of the cooling characteristics of the metallic-tube-cooled structure of C/C composite.[23] Figure 19 shows a test piece of the C/C composite inner shell. Laminate type 2D-C/C composite material was used. The inner shell of the C/C composite has 8 hemicircular grooves which encase the stainless steel cooling tubes. No damage and no discoloration on the surface of the stainless steel cooling tubes were observed after the heating test.

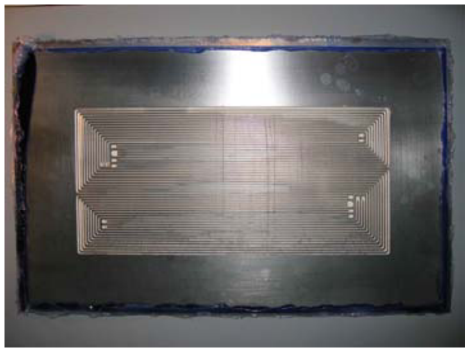

FIG 16. A stainless steel panel with cooling passages by chemical etching method.

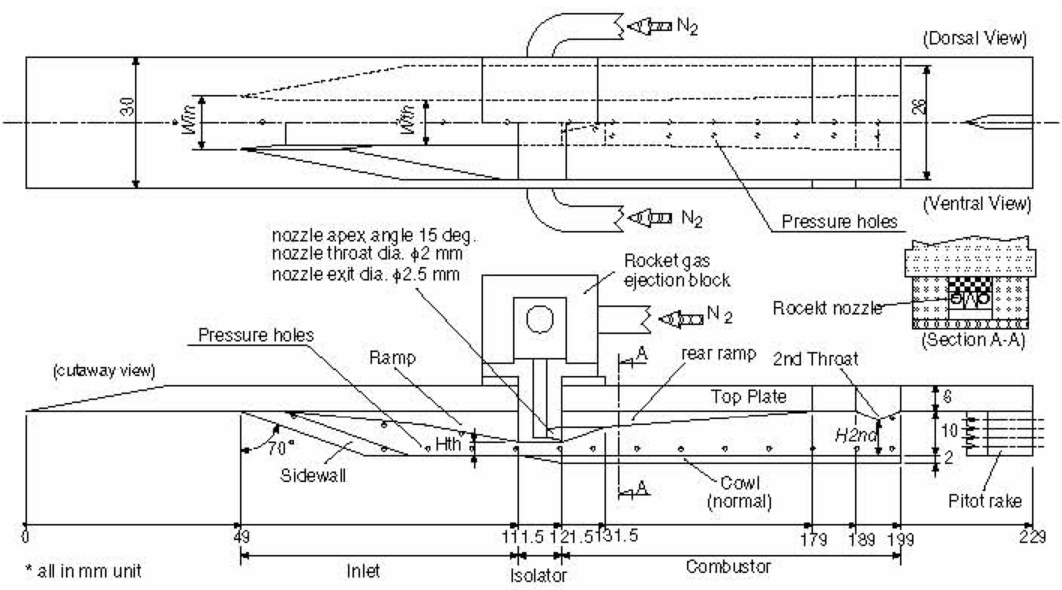

FIG 15. Engine model for transonic wind tunnel tests.

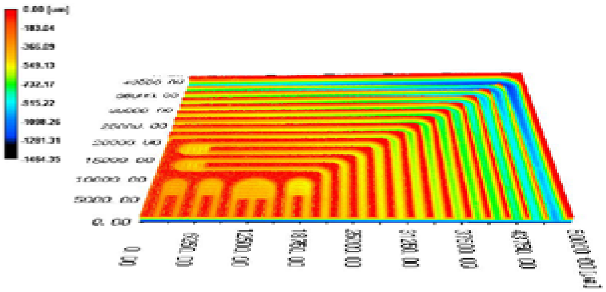

FIG 17. A stainless steel panel with cooling passages by chemical etching method.

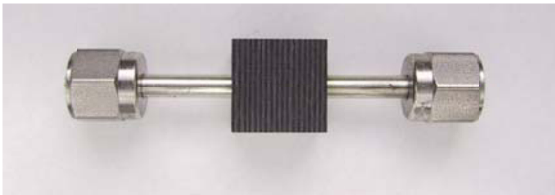

FIG 18. A specimen for evaluation test of cooling performance.

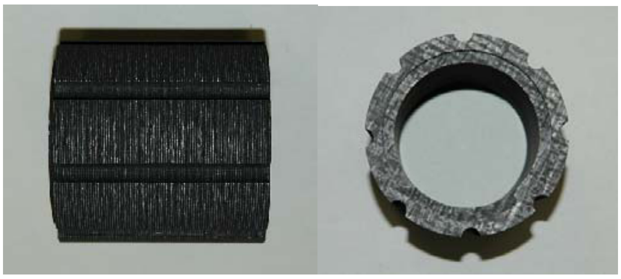

FIG 19. Test piece of C/C composite inner shell.

5.2. Thermo-Aerodynamics for Re-entry

Studies for re-entry vehicle are also being conducted[24] in HIEST, which can simulate re-entry condition. A direct acceleration measurement technique was developed by CALSPAN in the 1960s. In this technique, test models were weakly restrained (suspended) with low stiffness support such as thin wires, allowing the effect of restorative force due to model support to be neglected within a short test period. However, this technique has the disadvantage of degrading measurement accuracy with messy oscillations. To improve this tecnique, the signal recovery technique was applied to aerodynamic force measurement in the free-piston shock tunnel HIEST. To evaluate the feasibility of the present technique, unsteady drag force measurement was performed with the HB-2 hypersonic standard model. The measurement results were compared with the results obtained with the aerodynamic force balance technique in HIEST. The results were also compared with the results obtained in a blow-down type hypersonic wind tunnel. The schematics of the HB-2 model used in this study are shown in Fig. 20. Figure 21 shows a comparison between the present measurement technique and the aerodynamic force balance technique, which was previously performed in HIEST. The figure clearly shows that the balance results still had heavy fluctuation, caused by irrelevant high frequency components. However the present method does offer a faster time response without high-frequency noise.

To evaluate the present measurement uncertainty, a comparison with other wind tunnel facilities was conducted as shown in Figure 22. In this comparison, reference data was used that had been obtained in the blow-down type hypersonic wind tunnel HWT1 located at JAXA Chofu. Since the Mach number and Reynold's number differed between the facilities, the viscous interaction parameter $M_{\infty}/\sqrt{\mathrm{Re}}$ was applied to compare the tunnel results. The uncertainty of the HWT1 results is less than 3%. On the other hand, the uncertainty of the HIEST is less than 6%. The number of data in HIEST was not enough to evaluate the uncertainty in detail. However, the figure shows that the results were 5% higher than that of HWT1 measurements.

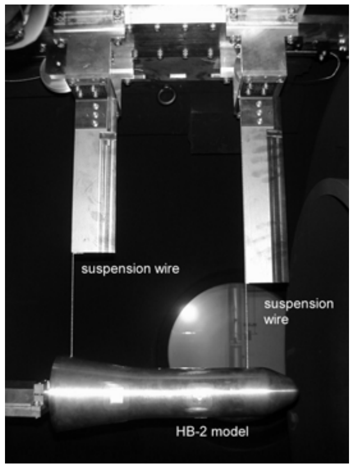

FIG 20. HB-2 standard model installed in the HIEST test section. The model was suspended from thin wires.

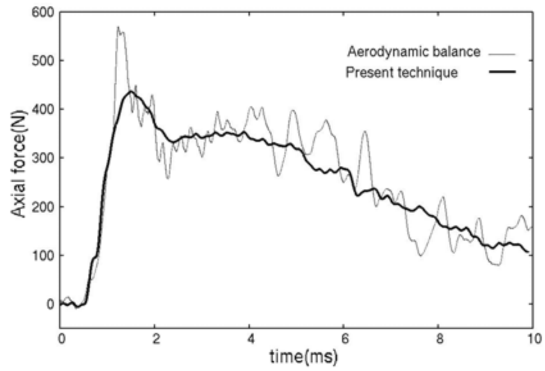

FIG 21. Axial force record of the HB-2 standard model.

6. SUMMARY

The Combined Propulsion Research Group of JAXA is conducting researches on the scramjet engine and the rocket-ramjet combined-cycle engine for wide applications of space transportation. In the scramjet engine research, net thrust was attained in lower Mach numbers and is being tested in higher Mach numbers. The scramjet is combined with the rocket engine to enlarge its operating range, and this rocket-ramjet combined- cycle engine is also studied. Based on results of component and system studies, sub-scale model was constructed and was tested. Researches on cooling panel and light-weight material are being progressed, which are necessary to realize the air-breathing new booster engine. Activities of thermo-aerodynamics on the re-entry vehicle are also progressed.

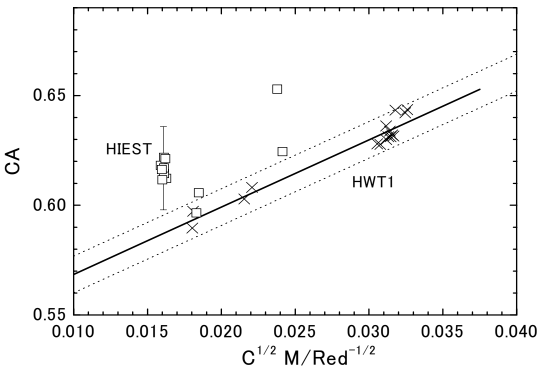

FIG 22. Comparison of the CA with viscous interaction parameter M/Re-1/2. The solid line shows the results obtained in HWT1. The dotted line shows 95% uncertainty. The open square shows the present results. The error bar shows 95% uncertainty.

7. REFERENCES

[1] Chinzei, N., “Reserach Activities on Scramjets at NAL-KRC in Japan,” 15th ISABE Paper 2001-1075, Bangalore, India, Sep. 2001.
[2] Hiraiwa, T., et al., “Recent Progress in Scramjet / Combined Cycle Engines at JAXA, Kakuda Space Propulsion Center,“ 57th IAC Paper IAC-06-C4.2.09, Valencia, Spain, Oct. 2006.
[3] Kanda, T., et al., “Design of Sub-Scale Rocket-Ramjet Combined-Cycle Engine Model,” 56th IAC Paper IAC-05-C4.5.03, Fukuoka, Japan, Oct. 2005.
[4] Kanda, T., et al., “Conceptual Study of a Combined-Cycle Engine for an Aerospace Plane,” Journal of Propulsion and Power, Vol. 19, No. 5, 2003, pp. 544-553.
[5] Kanda, T., et al., “Conceptual Study of a Rocket-Ramjet Combined-Cycle Engine,” 17th ISABE Paper 2005-1298, Munich, Germany, Sep. 2005.
[6] Masuya, G., et al., “A Study of Air Breathing Rockets – Subsonic Mode Combustion,” Acta Astronautica, No. 8, 1981, pp. 643-661.
[7] Kanda, T., et al., “Evaluation of Effectiveness of Periodic Flight by a Hypersonic Vehicle,” Journal of Aircraft (to be published.)
[8] Ueda, S., et al., “Mach 6 Test of a Scramjet Engine with Multi-Staged Fuel Injection,” AIAA Paper 2005-1027, Jan. 2006.
[9] Ueda, S., et al., “Performance Comparison of Combined Fuel Injection Methods in a Staged-Combustion Scramjet Engine,“ Proc. 25th ISTS, pp. 121-126, 2006.
[10] Kouchi, T., et al., “Transition of Combustion Modes in a Scramjet Engine,” 25th ISTS Paper ISTS-2006-a-46, Kanazawa, Japan, Jun. 2006.
[11] Takahashi, M., et al., “Experimental Study on Scramjet Engine Performance at Mach 10 to 15 Flight Condition,” 17th ISABE Paper 2005-1238, Munich, Germany, Sep. 2005.
[12] Takahashi, M., et al., “Effect of Combustor Shape on Scramjet Characteristics at Hypervelocity Condition over Mach 10 Flight,” AIAA Paper 2006-8024, Nov. 2006.
[13] Tomioka, S., et al., “Sea-level Static Tests of a Rocket-Ramjet Combined Cycle Engine Model,“ AIAA Paper 2007-5389, Jul. 2007.
[14] Takegoshi, M., et al., “Clustered Rocket Chamber for Rocket-Ramjet Combined Cycle Engine,“ ISABE 2007 (to be presented.)
[15] Kanda, T., et al., “Experimental Study of a Combined-Cycle Engine Combustor in Ejector-Jet Mode,” AIAA Paper 2006-0223, Jan. 2006.
[16] Kato, K., et al., “Preliminary Tests of Downstream Combustion Ramjet-Mode in a Combined Cycle Engine Combustor,” 25th ISTS Paper ISTS-2006-a-53, Kanazawa, Japan, Jun. 2006.
[17] Tani, K., et al., ``Designing and Aerodynamic Performance of the Combined-Cycle Engine Inlet in a Hypersonic Flow," 56th IAC Paper IAC-05-C4.5.06, Fukuoka, Japan, Oct. 2005.
[18] Tani, K., et al., “Aerodynamic Characteristics of the Modified Combined Cycle Engines“in Ejector-Jet Mode,” AIAA Paper 2006-0224, Jan. 2006.
[19] Saito, T., et al., "Experimental study of an etching method as a fabrication technique of cooling passages for combined cycle engine wall structure," 25th ISTS Paper ISTS-2006-c-03, Kanazawa, Japan, Jun. 2006.
[20] Saito, T., et al., “Experimental Study on Etching Method for Fabricating Cooling Passages in Combined-cycle-engine Wall,“ AIAA Paper 2007-2255, Apr. 2007.
[21] Takegoshi, M. and Ueda, S., “Cooling Characteristics of C/C Composite Material Structure with a Metallic Tube Fixed by Elastic Force of Each Material,” Journal of Japan. Soc. Aeronaut. Space Sci. 54, (2006), pp.129-135. (in Japanese).
[22] Takegoshi, M., et al., “Fundamental Study on Cooling Structure of C/C Composite Material with a Metalic Tube,“ 25th ISTS Paper ISTS-2006-c-04, Kanazawa, Japan, Jun. 2006.
[23] Takegoshi, M., et al., “Evaluation of Metallic-tube-cooled C/C Composite Structure by Rocket Combuster,“ AIAA Paper 2007-2357, Apr. 2007.
[24] Tanno, H., et al., “ Free-flight force Improvement technique in the impulsive facility HIEST,“ 22nd ICIASF, Jun. 2007.